Journal of Applied Physics

Reduced photothermal heating in diamonds enriched with H3 point defects

Cite as: J. Appl. Phys. **131**, 234401 (2022); https://doi.org/10.1063/5.0090661
Submitted: 08 March 2022 • Accepted: 10 May 2022 • Published Online: 16 June 2022

Anupum Pant, Chaman Gupta, Katharina Senkalla, et al.

AIP Publishing

Journal of Applied Physics ARTICLE scitation.org/journal/jap

Reduced photothermal heating in diamonds enriched with H3 point defects

Cite as: J. Appl. Phys. **131**, 234401 (2022); doi: 10.1063/5.0090661
Submitted: 8 March 2022 · Accepted: 10 May 2022 ·
Published Online: 16 June 2022

View Online Export Citation CrossMark

Anupum Pant,[1] Chaman Gupta,[1] Katharina Senkalla,[2] Greg Felsted,[3] Xiaojing Xia,[4] Tobias Spohn,[2] Scott T. Dunham,[5] Fedor Jelezko,[2] and Peter J. Pauzauskie[1,6,a)]

AFFILIATIONS

[1]Department of Materials Science and Engineering, University of Washington, Seattle, Washington 98195, USA
[2]Institute for Quantum Optics, Ulm University, Albert-Einstein-Allee 11, 89081 Ulm, Germany
[3]Department of Chemistry, University of Washington, Seattle, Washington 98195, USA
[4]Molecular Engineering & Sciences Institute, University of Washington, Seattle, Washington 98195, USA
[5]Department of Electrical and Computer Engineering, University of Washington, Seattle, Washington 98195, USA
[6]Physical & Computational Sciences Directorate, Pacific Northwest National Laboratory, Richland, Washington 99354, USA

[a)]**Author to whom correspondence should be addressed:** peterpz@uw.edu

ABSTRACT

Solid-state laser refrigeration of semiconductors remains an outstanding experimental challenge. In this work, we show that, following excitation with a laser wavelength of 532 nm, bulk diamond crystals doped with H3 centers both emit efficient up-conversion (anti-Stokes) photoluminescence and also show significantly reduced photothermal heating relative to crystals doped with nitrogen–vacancy (NV) centers. The H3 center in diamond is a highly photostable defect that avoids bleaching at high laser irradiances of 10–70 MW/cm^2 and has been shown to exhibit laser action, tunable over the visible band of 500–600 nm. The observed reduction of photothermal heating arises due to a decrease in the concentration of absorbing point defects, including NV-centers. These results encourage future exploration of techniques for H3 enrichment in diamonds under high-pressure, high-temperature conditions for the simultaneous anti-Stokes fluorescence cooling and radiation balanced lasing in semiconductor materials. Reducing photothermal heating in diamond through the formation of H3 centers also opens up new possibilities in quantum sensing via optically detected magnetic resonance spectroscopy at ambient conditions.

I. INTRODUCTION

Photothermal heating in nanodiamond materials[1] has created challenges for quantum sensing measurements based on optically detected magnetic resonance,[2,3] including scenarios when nanodiamonds are optically trapped in high vacuum conditions.[4] Recently, progress has been made in reducing photothermal heating in diamond materials grown via high-purity chemical vapor deposition (CVD);[5] however, CVD methods are difficult to apply to diamonds grown at high-pressure, high-temperature (HPHT) conditions. Currently, there is significant interest in developing solid-state laser refrigeration[6] materials that can mitigate detrimental photothermal heating for future applications in cavity optomechanics,[7,8] biophysics,[9,10] and quantum information science and technology.[11,12] In addition to band-to-band transitions and Auger emission from semiconductors,[13] dipole transitions from point defects in semiconductors, including both the negatively charged nitrogen–vacancy (NV) center[10] and the nitrogen–vacancy–nitrogen (H3) center[11] in diamond, have been proposed recently as potential candidates for solid-state laser cooling. However, to date, the experimental demonstration of solid-state laser cooling of semiconductors remains a longstanding experimental challenge.[13–15]

The H3 center in diamond exhibits several promising characteristics[16,17] for laser cooling applications including a neutral charge state, a high radiative quantum yield ∼ 95%,[18] a long excited-state lifetime (∼17 ns), and efficient anti-Stokes photoluminescence[19] that make it a potential candidate for demonstrating solid-state laser cooling of diamond. The H3 center consists of a nitrogen–vacancy–nitrogen (NVN) complex with C_{2v} rotational symmetry along ⟨111⟩ zone axes within diamond's FCC Bravais lattice [Fig. 1(e)]. Its characteristic emission features consist of a prominent zero-phonon line (ZPL) at 503 nm with the corresponding wide phonon sidebands (PSBs) red-shifted from the ZPL. Its photostability and high quantum efficiency

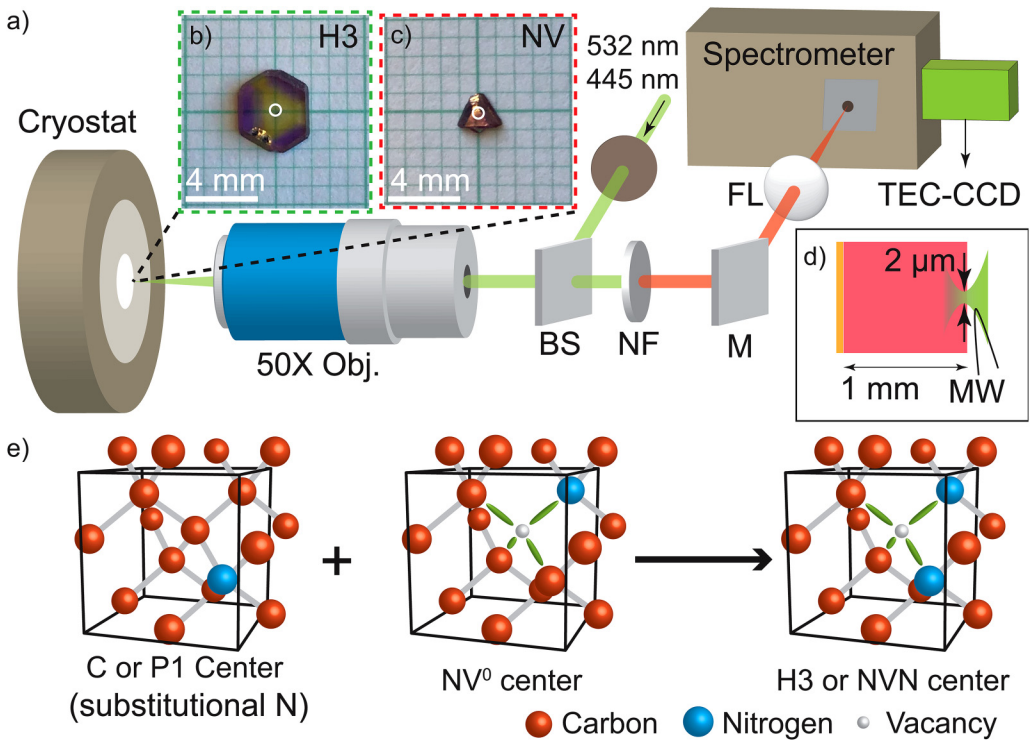

FIG. 1. (a) The optical setup for the excitation of the diamond sample using a focused 532 or 445 nm laser spot. The backscattered part of the emission is collected using the 50× long working distance objective (50× obj.), transmitted through a beam-splitter (BS), filtered using a notch filter (NF) or a long-pass filter, reflected using a mirror (M), and focused into the spectrometer slit using a focusing lens (FL). A thermo-electrically cooled charge-coupled device (TEC-CCD) was used to record the spectrum. (b) The H3 diamond sample with predominant nitrogen doping in the form of NVN or H3 centers, and (c) the NV diamond with predominantly NV centers. The white circle represents the area where the 532 nm spot was focused on the respective diamond. (d) The side-view schematic of a diamond sitting on a quartz coverslip. (e) A schematic showing the mobilization of NV and integration of substitutional nitrogen (C-centers or P1 centers) with NV^0 centers at high pressures and temperatures to form NVN or H3 centers.

have also been used to report tunable laser action in the visible spectral region between 500 and 600 nm.[18] In this work, we demonstrate both efficient anti-Stokes emission from the H3 center and also reduced photothermal heating in macroscopic HPHT diamonds that have been enriched with H3 centers relative to control samples containing NV centers. We hypothesize that the reduced heating is due to the depletion of nitrogen-related defects (including NV and P1 centers) within the crystal, leading to reduced background absorption of the bulk diamond crystal lattice.

II. MATERIALS AND METHODS

Figure 1(a) depicts an experimental optical setup designed to collect the emission from macroscopic diamond crystals excited locally to investigate the photothermal properties of the H3 center. Two diamond samples were studied, one enriched with H3 centers [Fig. 1(b)] using the technique reported by Rand *et al.*[18] and the other grown with a high concentration of NV centers [Fig. 1(c)]. The mechanism with which the H3-centers are formed in a diamond is shown in Fig. 1(e). The H3 diamond was treated at high-pressure and high-temperature conditions[18] under which the NV^0 centers become mobile and form the NVN (H3) center through recombination with P1 defects.[20]

The diamond sample shown in Fig. 1(b) was hexagonal-shaped and predominantly contained point defects in the form of H3-centers (NVN-centers). It was yellow-colored around the center of the crystal, while the areas away from the center had a red/purple hue. The area with the red/purple hue was observed to have a higher proportion of NV^0 and NV^- centers. For these experiments, the central area (white circle), which is shown to have a high proportion of H3 center to other defects, was used. The second sample shown in Fig. 1(c) was triangular-shaped and had a bright red/purple hue overall due to a high concentration of NV centers. The samples were fixed to a Janis ST 500 cryostat's stage using a double-side copper tape. The focal spot of the lasers was maintained $\sim 10\,\mu$m below the top surface of the diamonds, and the focal volume heated and probed using the lasers was approximated to be less than $100\,\mu m^3$. Given the large absorption coefficient and thickness of the diamond compared to the laser spot size, the divergent beam reaching the lower part of the diamond substrate had a low irradiance, which resulted in negligible photothermal heating of the copper tape.

The optical setup for the excitation of the diamond sample uses focused continuous-wave lasers with wavelengths of either 532 nm (Coherent Sapphire LP) or 445 nm (HJ Optronics OEM-SD-445). A 50X-Mitutoyo infinity-corrected, long working distance (13 mm) objective lens with a 0.55 numerical aperture was used to focus and collect the emission from the diamond. To get rid of the scattered laser light, transmitted light from the 70/30 beam-splitter (BS) was filtered using a 532 nm notch filter (NF) and a 475 nm long-pass filter. The emission was then reflected using a mirror (M) and focused into the spectrometer slit using a plano–convex focusing lens (FL). ProEM 512, a thermoelectrically cooled charge-coupled device (TEC-CCD), and Blaze-100HR from Princeton Instruments was used to record the spectra along with a Princeton Instruments HRS-500. Lifetime measurements were performed using EPL-450, a pulsed 450 nm excitation laser from Edinburgh Instruments. An Avalance Photo-Diode (APD) from OptoElectronics Components PDM Module was used to perform single-photon counting.

To conduct the optically detected magnetic resonance (ODMR) experiments, a 20 μm thick insulated copper wire loop was used as an antenna to apply varying microwave frequencies within the NV-enriched diamond. The ODMR was performed using a home-built optical microscope setup. The NV^- centers were excited using a single longitudinal mode 532 nm laser (Coherent Sapphire LP). The microwaves were generated using a Windfreak SynthHD Pro Microwave Generator. The NV^- center emission was collected using a single-photon counting avalanche photodiode (Excelitas SPCM-AQRH). All data analysis and processing were performed using in-house developed Python scripts.

III. RESULTS AND DISCUSSION

The Stokes part of the emission spectra was collected from the H3 and NV diamonds under laser excitation of 532 nm excitation as shown in black and red in Fig. 2(a), respectively. The emission wavelength of NV^0 and NV^- ZPLs are marked using yellow and red dashed lines centered at 575 and 638 nm, respectively. The counts are normalized using the laser power used and the acquisition time. The integrated emission intensity from NV-centers from the NV diamond sample was measured to be 11 times higher relative to NV-emission from the H3 diamond. This more intense NV emission indicates a higher concentration of NV centers present within the NV diamond in comparison with the H3 sample. The inset of Fig. 2(a) shows the modulation in the emission intensity from the NV diamond using a microwave (MW) frequency sweep from 2.86 to 2.88 GHz. Stronger emission from the excited state to the ground state is seen when the NV^- center is in the $m_s = 0$ state (vs the lower emission when the MW is resonant with the $m_s = \pm 1$ states). The weaker emission associated with $m_s = \pm 1$ results from a stronger non-radiative coupling to the singlet energy level through the intersystem crossing. The splitting in $m_s = \pm 1$ (weakest emission) states is due to the combination of local magnetic field and strains within the sample.

The anti-Stokes part of emission spectra collected from the H3 and NV diamonds using a 532 nm excitation is shown in black and red in Fig. 2(b), respectively. Strong anti-Stokes emission from H3 centers is observed in the H3 diamond, while it is absent in the

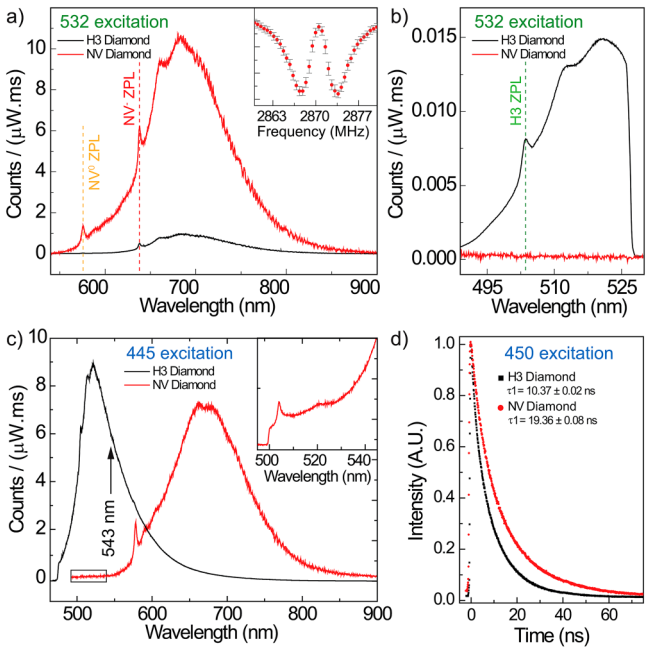

FIG. 2. (a) Normalized room temperature spectra of NV^0 and NV^- emission from both H3 (black) and NV (red) samples using a 1 mW 532 nm laser excitation spot. The inset shows the ODMR spectrum measured from the NV diamond. (b) The anti-Stokes wavelength band spectra for both the H3 (black) and NV (red) samples using 532 nm excitation. (c) Normalized room temperature full-range spectra using a 445 nm laser excitation spot. The inset shows a zoom-in view of the H3 center signal in the NV diamond sample. (d) Measured and exponential fitted lifetime data for H3 sample (black) and NV sample (red) with a 450 nm excitation.

NV diamond. Green dashed line shows the H3 ZPL center wavelength at 503 nm with the red-shifted wide Gaussian phonon sidebands. The presence of anti-Stokes fluorescence is important for realizing solid-state laser refrigeration and motivates conducting experiments in the future to evaluate the efficiency of this process at different excitation wavelengths. The spectra were cut off at 527 nm due to the notch filter used to remove the scattered 532 nm laser.

The Stokes part of emission spectra from the H3 and NV diamond spots measured using a focused 445 nm laser excitation is shown in Fig. 2(c) for both H3 (black) and NV (red) samples, respectively. Emission from the H3 diamond predominantly consists of emission from the H3 ZPL at 503 nm and a broad phonon overtone emission with a center around 530 nm, representing a relatively high concentration of H3 centers in the sample. The instrument-induced intensity variation with wavelength was corrected using a calibrated halogen lamp to obtain the mean wavelength. A Jacobian transformation was applied following Mooney *et al.*[21] to convert the intensity vs wavelength data into intensity vs energy. The frequency centroid was calculated to obtain the mean emission energy ($\bar{E} = h\bar{\nu}$) of 2.28 eV. This mean emission frequency corresponds to the mean wavelength ($\bar{\lambda} = c/\bar{\nu}$) of

543.71 nm. Details about this method for mean fluorescence energy calculation are provided in the supplementary material. A 475 nm long-pass filter was used to block the laser signal from entering the spectrometer, which resulted in a cut-off in the emission signal from the H3 diamond sample. Statistical fitting was performed to extrapolate the signal on the blue side of 475 nm as shown in the supplementary material Fig. 2. This is important for laser refrigeration applications as only wavelengths red-shifted to this wavelength can be used to observe the net cooling of diamonds through H3 centers doped in them.

While Fig. 2(c) shows no NV emission from the H3 diamond when the pump laser was focused tightly within an area with a low NV concentration, emissions from NV centers are observed when the entire crystal is optically excited (supplementary material Fig. 4). Supplementary material Fig. 5 shows photoluminescence excitation (PLE) spectra of the H3 diamond collected at 530 and 680 nm, which are the emission wavelengths with the highest intensity of the phonon sidebands of the H3 and NV centers, respectively. The PLE spectra confirm the presence of NV centers in the H3 diamond, as well as other point defects that likely contribute to background absorption. Two-photon absorption can also contribute to the emission from H3 diamond. However, it has been predicted to be quite weak as shown by Lin *et al.*[16] and will have a different power dependency compared to the anti-Stokes emission.

As can be seen in Fig. 2(c), for an excitation wavelength of 445 nm, the emission from the NV diamond predominantly consists of the NV^0 ZPL at 575 nm and a broad phonon overtone centered around 680 nm. The weak NV^- ZPL emission at 638 nm is due to the strong photo-ionization of NV^- centers to NV^0 using the 445 nm laser. The emission from the NV sample primarily occurred due to the NV centers where a large fraction of the emission intensity (~36.3%) was contributed by NV^0, indicating an efficient ionization of NV^- due to the high energy of the incident laser (445 nm). A very small amount of emission intensity in the NV diamond was from the H3 center due to the very low concentration of the H3 centers in this sample. This is indicated using a gray box and the close-up is shown as an inset in Fig. 2(c).

Lifetime measurements using an unfocused, pulsed 450 nm excitation laser were conducted on the H3 diamond with detection window centers both at 530 nm (maximum of H3 center phonon overtone emission) and 680 nm (maximum of NV^- center phonon overtones) as shown in Fig. 2(d). Double exponential fitting to the 530 nm band decay spectrum shows 10.37 and 2.41 ns decay components. The time scales are smaller than the intrinsic H3 lifetimes of ~ 16.7 ns.[22] The short decay time component (2.41 ns) can be attributed to the heavy quenching of H3 luminescence by other luminescent defects. Since an H3 center is created from an A-aggregate plus a vacancy, or NV centers and P1 centers, spatial correlations are likely between the H3 centers and the A-aggregates, or NV centers.[23] The A-aggregates act as quenching centers, decreasing the lifetime of H3 ensembles in closer proximity to them.[23] No NV^- or NV^0 luminescence could be observed at the center of the H3 diamond, where the lifetime measurements were performed. However, NV^- luminescence could be observed when the 450 nm laser was focused near the edge of the H3 diamond. The NV^- emission from this region shows a rise and a decay component with time scales of 5.8 and 16.9 ns, corresponding to the

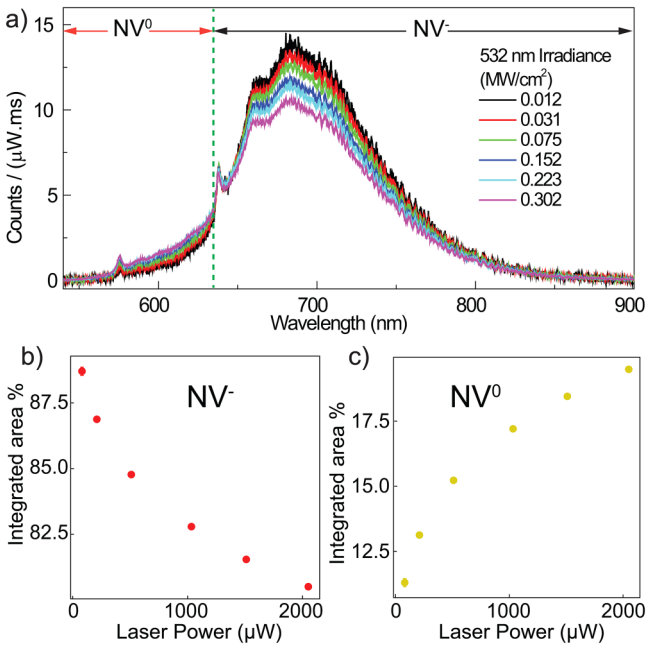

FIG. 3. (a) Room temperature normalized emission spectra from the NV diamond sample at six different 532 nm irradiances. (b) Area percentage under intensity curves of (b) NV^- and (c) NV^0 emission intensity at the six different irradiances from the ZPL and overtones fit.

excitation of the NV centers from the trapped H3 emission (similar to re-absorption and photon recycling effects in perovskite materials[24]) and the intrinsic NV^- center lifetime, respectively. The lifetime of emission from the 680 ± 10 nm phonon overtone from the NV diamond sample was fit to a double exponential with decay times of 19.36 and 7.4 ns. The 19.36 ns lifetime is much longer than the intrinsic lifetime of the NV^- center (12–13.5 ns[25,26]) but close to the 21 ns intrinsic lifetime of the NV^0 center. The high emission percentage from the NV^0 in the NV diamond sample's spectrum due to blue light excitation as seen in Fig. 2(c) may contribute to these long time scales.

The room temperature emission spectra of the NV diamond sample were measured at six different laser irradiances and shown in Fig. 3(a). The measured counts normalized using the laser power and acquisition times are shown on the y axis with units of counts/(μW ms). The vertical green dotted line signifies an arbitrary separation of the emission spectra such that the left and right sides indicated using red and black lines represent the wavelength ranges in which the predominant amount of emission originates from the NV^0 center and NV^-, respectively. However, since the phonon overtones from the NV^0 are convoluted with the NV^-, a more sophisticated technique is required to measure the percentage of emission from the NV^0 as compared to the total emission. To calculate this, the method of fitting several spectra for the NV^0 and NV^- ZPLs and the overtones described in the supplementary material was used. The sum of amplitudes of the L_2 and $G_6 - G_9$, as shown in the supplementary material Fig. 1 fit the normalized

spectra gave the emission from the NV^0 centers. The sum of amplitudes from fits of all the other peaks contributes to the emission from the NV^- centers. The percentage of the respective charge state emission from NV^- and NV^0 was calculated and is plotted in Figs. 3(b) and 3(c), respectively. At higher irradiances, NV^- is dynamically ionized to NV^0 (and back) at a faster rate,[27] causing the relative percentage of emission from NV^0 to rise from 12 to 18% as the laser power increases from 81 to 2050 μW. The decrease in dynamic population of the NV^- suggests that the absorption by NV^- would progressively become smaller at higher irradiances as shown by Subedi *et al.*[28]

To calculate the Debye–Waller Factor (DWF), the area under the ZPL (I_1) was obtained by fitting the spectrum in a narrow wavelength range of around the 638 nm using a composite function consisting of a linear background and a Lorentzian. The amplitude of the Lorentzian is I_1. A representative fit for the ZPL using the composite function is shown using a red fill in Fig. 4(a). The area under the phonon sidebands (I_2) can be obtained by integrating over the spectrum and subtracting the previously determined ZPL area from it. The DWF is calculated by taking the ratio I_1 to I_2. The change in DWF with temperature has been reported by Plakhotnik *et al.*[29] Accurate temperature measurements using

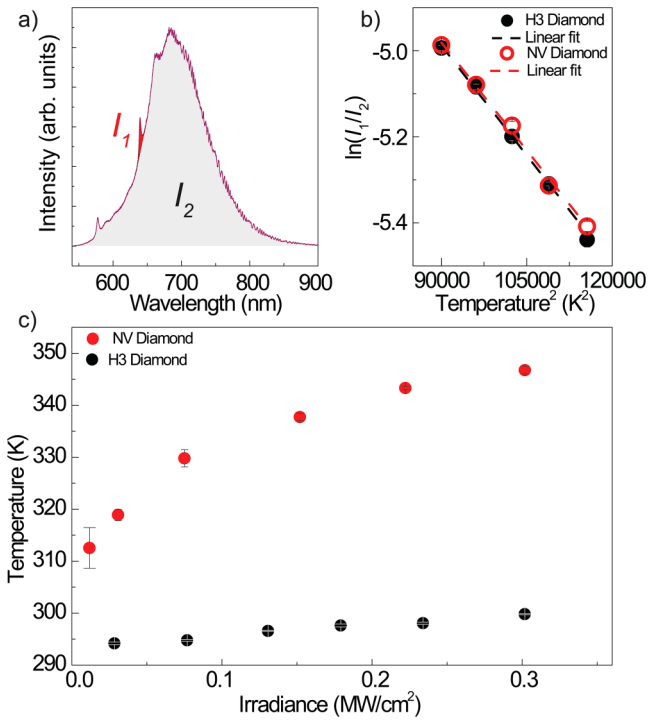

FIG. 4. (a) PL emission using 532 excitation source from NV diamond with area under NV^- ZPL marked as I_1 and area under phonon-sidebands marked as I_2. (b) DWF temperature calibrations for the H3 and NV diamond samples shown with black filled and red unfilled circles, respectively. Dashed line corresponds to the best linear fit. (c) Irradiance dependent calibrated temperatures for the H3 (black circles) and NV (red circles) diamond samples.

ODMR required precise detection of frequency shifts of at least 1.3 MHz for the NV diamond sample and 200 kHz for the H3 diamond sample.[30] Due to high sample strain and other paramagnetic defects, linewidths of the dips obtained in the ODMR signal from both the samples were not sharp enough to precisely measure the temperature changes. Therefore, DWF was chosen over ODMR as the thermometry technique. Moreover, using the DWF thermometry, one can avoid the need for microwave equipment in future laser cooling experiments.

The temperature-dependent measurement of the DWF for the H3 diamond was done using a laser irradiance of 12 kW/cm^2 at a wavelength of 532 nm. A fit to the DWF equation is shown using a black dashed line [Fig. 4(b)], which gives the Debye temperature $T_D = 1133.7$ K and the electron–phonon coupling parameter $S = 3.41$. The same measurement was repeated on the NV diamond. The fit to the DWF equation shown using a red dashed line [Fig. 4(b)] gives $T_D = 1164.3$ K and $S = 3.46$. These values were used to calibrate the laser irradiance-dependent measurements to obtain the change in temperature as shown in Fig. 4(c). The calibrations were validated by comparing the calibrations curves of various laser power levels. The slopes of each curve were compared for any nonlinearity or deviation based on the power level as shown in the supplementary material Fig. 6. No such deviation was observed, suggesting that the calibrations done are valid for all laser powers used in this experiment. The overall temperature change near the laser spot in the H3 diamond is close to 5 K at the highest irradiance. However, at the same laser irradiance, the NV diamond heats to temperatures 50 K higher than room temperature. Note that the NV diamond sample does not heat linearly with the increase in laser irradiance, as one would expect for materials with a constant absorption coefficient at a particular wavelength. As the excitation laser irradiance is increased, it is likely that the absorption coefficient decreases due to a decrease in the population of the NV^-, as observed in the previous figures.

Similarly, the 10-fold decrease in photothermal heating of the H3 diamond can be attributed to the significantly smaller amount of NV centers in the sample as discussed above. This is encouraging for further exploration of methods to convert NV centers to H3 centers in a diamond sample. The ability to maintain a relatively high stable population of H3 centers in a sample may result in minimized heating which is advantageous considering its possible applications as a lasing medium. Additionally, the presence of anti-Stokes emission from the H3 center motivates its further exploration as a laser refrigeration color center for radiation-balanced lasers.

As noted above, H3 centers can be formed by heating samples with NV centers at temperatures high enough to enable their diffusion. The NV dissociation energy is higher than the migration energy, so NVs diffuse as a complex, limited by the nearly equal barriers (4.8–4.85 eV) calculated for N/V exchange and realignment via the V moving away to 3NN (3rd nearest neighbor) distance and returning along a different path.[20] In order to optimize this process for laser cooling, it is critical that nearly all NV centers are transformed to H3 centers via binding with substitutional N (N_C). This can be achieved by using long-time, high-temperature anneals in systems with high substitutional N concentrations.

Both theory[20,31] and experiment[21,32] indicate that temperatures above about 1500°C are required to activate NV diffusion.

Extrapolating the hopping rate calculated by Chakravarthi *et al.*[32] (which closely aligns with the theoretical value) combined with a diffusion-limited reaction rate and moderate range capture distance (~4 NN) leads to an estimate for the time constant of NV transformation to H3 via capture by N_C of about 2 h at 1600°C for a substitutional N concentration of 1000 ppm (with proportionally longer required for lower N_C concentrations). Once formed, the stability of H3 centers is limited by the dissociation into A-centers and vacancies ($N_2 + V_C$). Theoretical calculations indicate a barrier of 6.5 eV for this process.[31] Assuming an effective attempt frequency of about 10 THz, this gives a dissolution rate of about 8 h at 1600°C. Thus, there appears to be a possible window for the formation of large densities of H3 defects via annealing of N-rich, NV-rich samples. Higher densities of H3 centers can be achieved at lower temperatures, with the trade-off being longer annealing times. For example, at 1500°C, the time constants for H3 formation (at 1000 ppm N) and decomposition would be about 11 and 80 h, respectively. To avoid graphitization at such high temperatures, especially for nanodiamond samples, it is desirable for annealing to take place at high pressures in the absence of oxygen, as can be achieved in diamond anvil cells or HPHT reactors. Point defect diffusion has also been reported to depend on the defect's charge state.[33] Consequently, Coulomb interactions may accelerate the formation of H3 centers from positively charged P1 centers and negatively charged NV centers.

An alternative route to the formation of H3 centers is irradiation and annealing of Type IaB diamond that already contains large numbers of N_2 complexes (A-centers).[16] However, while the H3 signature can be observed in these materials, there are also large concentrations of other competing complexes, including NV, N_3V (N3 centers), N_4V (B-centers), and N_4V_2 (H4) complexes.[21] It has also been found that the H3 emission is quenched by the large density of N aggregates in such materials.[34] Future work will be focused on the synthesis and laser cooling of diamond materials with high concentrations of H3 centers.

SUPPLEMENTARY MATERIAL

See the supplementary material for additional details on methods for data analysis.

ACKNOWLEDGMENTS

A.P., X.X., C.G., and P.J.P. gratefully acknowledge financial support from the MURI:MARBLe project under the auspices of the Air Force Office of Scientific Research (Award No. FA9550-16-1-0362). S.T.D. and P.J.P. also acknowledge support from the National Science Foundation and the UW Molecular Engineering Materials Center, a Materials Research Science and Engineering Center (No. DMR-1719797). The authors gratefully acknowledge Stephen Rand for providing the diamond samples used in this study. Sample characterization was conducted at the University of Washington Molecular Analysis Facility, which is supported in part by the National Science Foundation (NSF) (Grant No. ECC-1542101), the University of Washington, the Molecular Engineering & Sciences Institute, the Clean Energy Institute, and the National Institutes of Health. P.J.P. acknowledges support from the Northwest Institute for Materials Physics, Chemistry, and Technology (NW-IMPACT).

AUTHOR DECLARATIONS

Conflict of Interest

The authors have no conflicts to disclose.

Author Contributions

A.P. and C.G. contributed equally to this work.

DATA AVAILABILITY

The data that support the findings of this study are available from the corresponding author upon reasonable request.

REFERENCES

[1]C. Laube, J. Hellweg, C. Sturm, J. Griebel, M. Grundmann, A. Kahnt, and B. Abel, "Photoinduced heating of graphitized nanodiamonds monitored by the Raman diamond peak," J. Phys. Chem. C **122**, 25685–25691 (2018).
[2]P. Neumann, I. Jakobi, F. Dolde, C. Burk, R. Reuter, G. Waldherr, J. Honert, T. Wolf, A. Brunner, J. H. Shim, D. Suter, H. Sumiya, J. Isoya, and J. Wrachtrup, "High-precision nanoscale temperature sensing using single defects in diamond," Nano. Lett. **13**, 2738–2742 (2013), arXiv:1304.0688.
[3]G. Kucsko, P. C. Maurer, N. Y. Yao, M. Kubo, H. J. Noh, P. K. Lo, H. Park, and M. D. Lukin, "Nanometre-scale thermometry in a living cell," Nature **500**, 54–58 (2013).
[4]T. Delord, L. Nicolas, M. Bodini, and G. Hétet, "Diamonds levitating in a Paul trap under vacuum: Measurements of laser-induced heating via NV center thermometry," Appl. Phys. Lett. **111**, 013101 (2017).
[5]A. C. Frangeskou, A. T. M. A. Rahman, L. Gines, S. Mandal, O. A. Williams, P. F. Barker, and G. W. Morley, "Pure nanodiamonds for levitated optomechanics in vacuum," New J. Phys. **20**, 043016 (2018).
[6]D. V. Seletskiy, S. D. Melgaard, S. Bigotta, A. Di Lieto, M. Tonelli, and M. Sheik-Bahae, "Laser cooling of solids to cryogenic temperatures," Nat. Photonics **4**, 161–164 (2010).
[7]A. Pant, X. Xia, E. J. Davis, and P. J. Pauzauskie, "Solid-state laser refrigeration of a composite semiconductor Yb:$YLiF_4$ optomechanical resonator," Nat. Commun. **11**, 3235 (2020).
[8]D. R. Luntz-Martin, R. G. Felsted, S. Dadras, P. J. Pauzauskie, and A. N. Vamivakas, "Laser refrigeration of optically levitated sodium yttrium fluoride nanocrystals," Opt. Lett. **46**, 3797–3800 (2021).
[9]P. B. Roder, B. E. Smith, X. Zhou, M. J. Crane, and P. J. Pauzauskie, "Laser refrigeration of hydrothermal nanocrystals in physiological media," Proc. Natl. Acad. Sci. U.S.A. **112**, 15024–15029 (2015).
[10]M. Kern, J. Jeske, D. W. M. Lau, A. D. Greentree, F. Jelezko, and J. Twamley, "Optical cryocooling of diamond," Phys. Rev. B **95**, 235306 (2017).
[11]X. Xia, A. Pant, A. S. Ganas, F. Jelezko, and P. J. Pauzauskie, "Quantum point defects for solid-state laser refrigeration," Adv. Mater. **33**, 1905406 (2021).
[12]A. Pant, R. G. Felsted, A. B. Bard, X. Xia, S. Dadras, K. Shayan, D. R. Luntz-Martin, D. Mannikko, I. M. Pavlovetc, S. Stoll, M. Kuno, A. N. Vamivakas, and P. J. Pauzauskie, "Solid-state laser refrigeration of nanodiamond quantum sensors," arXiv:2007.15247[cond-mat.mtrl-sci] (2020).
[13]M. Sheik-Bahae and R. I. Epstein, "Can laser light cool semiconductors?," Phys. Rev. Lett. **92**, 247403 (2004).
[14]H. Gauck, M. Renn, E. Cornell, and K. Bertness, "Laser refrigeration in the solid state," in *Quantum Electronics and Laser Science Conference* (Optical Society of America, 1995), p. QPD16.
[15]Y. V. Morozov, S. Zhang, A. Pant, B. Jankó, S. D. Melgaard, D. A. Bender, P. J. Pauzauskie, and M. Kuno, "Can lasers really refrigerate CdS nanobelts?," Nature **570**, E60–E61 (2019).

[16]C. K. Lin, H. C. Chang, M. Hayashi, and S. H. Lin, "Excitation properties of the H3 defect center in diamond: A theoretical study," Chem. Phys. Lett. **475**, 68–72 (2009).
[17]R. Kolesov, S. Lasse, C. Rothfuchs, A. D. Wieck, K. Xia, T. Kornher, and J. Wrachtrup, "Superresolution microscopy of single rare-earth emitters in YAG and H3 centers in diamond," Phys. Rev. Lett. **120**, 033903 (2018).
[18]S. Rand and L. DeShazer, "Visible color-center laser in diamond," Opt. Lett. **10**, 481–483 (1985).
[19]T. T. Tran, B. Regan, E. A. Ekimov, Z. Mu, Y. Zhou, W.-b. Gao, P. Narang, A. S. Solntsev, M. Toth, I. Aharonovich, and C. Bradac, "Anti-Stokes excitation of solid-state quantum emitters for nanoscale thermometry," Sci. Adv. **5**, eaav9180 (2019).
[20]H. Pinto, R. Jones, D. Palmer, J. Goss, P. Briddon, and S. Öberg, "On the diffusion of NV defects in diamond," Phys. Status Solidi A **209**, 1765–1768 (2012).
[21]M. N. R. Ashfold, J. P. Goss, B. L. Green, P. W. May, M. E. Newton, and C. V. Peaker, "Nitrogen in diamond," Chem. Rev. **120**, 5745–5794 (2020).
[22]M. Thomaz and G. Davies, "The decay time of N3 luminescence in natural diamond," Proc. R. Soc. A **362**, 405–419 (1978).
[23]G. Liaugaudas, A. T. Collins, K. Suhling, G. Davies, and R. Heintzmann, "Luminescence-lifetime mapping in diamond," J. Phys. Condens. Matter **21**, 364210 (2009).
[24]H. Diab, C. Arnold, F. Lédée, G. Trippé-Allard, G. Delport, C. Vilar, F. Bretenaker, J. Barjon, J.-S. Lauret, E. Deleporte *et al.*, "Impact of reabsorption on the emission spectra and recombination dynamics of hybrid perovskite single crystals," J. Phys. Chem. Lett. **8**, 2977–2983 (2017).
[25]A. Collins, M. Thomaz, and M. I. B. Jorge, "Luminescence decay time of the 1.945 eV centre in type ib diamond," J. Phys. C Solid State Phys. **16**, 2177 (1983).
[26]A. Batalov, C. Zierl, T. Gaebel, P. Neumann, I.-Y. Chan, G. Balasubramanian, P. Hemmer, F. Jelezko, and J. Wrachtrup, "Temporal coherence of photons emitted by single nitrogen-vacancy defect centers in diamond using optical Rabi-oscillations," Phys. Rev. Lett. **100**, 077401 (2008).
[27]N. Aslam, G. Waldherr, P. Neumann, F. Jelezko, and J. Wrachtrup, "Photo-induced ionization dynamics of the nitrogen vacancy defect in diamond investigated by single-shot charge state detection," New J. Phys. **15**, 013064 (2013).
[28]S. D. Subedi, V. V. Fedorov, J. Peppers, D. V. Martyshkin, S. B. Mirov, L. Shao, and M. Loncar, "Laser spectroscopic characterization of negatively charged nitrogen-vacancy (NV^-) centers in diamond," Optics Mater. Express **9**, 2076–2087 (2019).
[29]T. Plakhotnik, M. W. Doherty, J. H. Cole, R. Chapman, and N. B. Manson, "All-optical thermometry and thermal properties of the optically detected spin resonances of the NV^--center in nanodiamond," Nano Lett. **14**, 4989–4996 (2014).
[30]D. M. Toyli, D. J. Christle, A. Alkauskas, B. B. Buckley, C. G. Van de Walle, and D. D. Awschalom, "Measurement and control of single nitrogen-vacancy center spins above 600 K," Phys. Rev. X **2**, 031001 (2012).
[31]R. Jones, J. P. Goss, H. Pinto, and D. W. Palmer, "Diffusion of nitrogen in diamond and the formation of A-centres," Diamond Relat. Mater. **53**, 35–39 (2015).
[32]S. Chakravarthi, C. Moore, A. Opsvig, C. Pederson, E. Hunt, A. Ivanov, I. Christen, S. Dunham, and K.-M. C. Fu, "Window into NV center kinetics via repeated annealing and spatial tracking of thousands of individual NV centers," Phys. Rev. Mater. **4**, 023402 (2020).
[33]P. Deák, B. Aradi, M. Kaviani, T. Frauenheim, and A. Gali, "Formation of NV centers in diamond: A theoretical study based on calculated transitions and migration of nitrogen and vacancy related defects," Phys. Rev. B **89**, 075203 (2014).
[34]M. D. Crossfield, G. Davies, A. T. Collins, and E. C. Lightowlers, "The role of defect interactions in reducing the decay time of H3 luminescence in diamond," J. Phys. C Solid State Phys. **7**, 1909–1917 (1974).